Mechanical and Functional Properties of Composites Based on Graphite and Carboxylated Acrylonitrile Butadiene Rubber

Jian Yang,[1] Li-Qun Zhang,[1,2] Jun-Hong Shi,[1] Yan-Nan Quan,[2] Lei-Lei Wang,[2] Ming Tian[1,2]

[1]*Key Laboratory of Carbon Fiber and Functional Polymers, Ministry of Education, Beijing, China 100029*
[2]*Key Laboratory of the Preparation and Processing of Novel Polymer Materials, Beijing University of Chemical Technology, Beijing, China 100029*

Received 4 July 2009; accepted 16 November 2009
DOI 10.1002/app.31792
Published online 27 January 2010 in Wiley InterScience (www.interscience.wiley.com).

ABSTRACT: In this study, carboxylated acrylonitrile butadiene rubber (xNBR)/expanded graphite (EG) nanocomposites were prepared with a latex compounding technique by ultrasonic stirring. The dispersion of EG in the xNBR matrix was investigated with transmission electron microscopy, scanning electron microscopy, and X-ray diffraction analysis. EG could be exfoliated into lots of nanosheets dispersing in the xNBR matrix. More EG loading resulted in the presence of a few incompletely exfoliated agglomerates. The mechanical properties (hardness, tensile modulus, and tensile strength) of the xNBR/EG composites were determined. Dynamic mechanical thermal analysis was also performed, and it showed that the nanosheets of EG somewhat immobilized the motion of rubber macromolecular chains and led to the shifting and broadening of the tan δ peak toward higher temperatures. Many other functional properties of EG-filled xNBR composites were studied, and it was established that the composites had excellent electrical conductivity as well as gas-barrier and wear properties. © 2010 Wiley Periodicals, Inc. J Appl Polym Sci 116: 2706–2713, 2010

Key words: barrier; composites; fillers; rubber

INTRODUCTION

Nanocomposites are defined as composite materials in which the reinforcement has at least one dimension in the range of 1–100 nm. The most commonly used nanoreinforcements are layered silicate nanoclays[1–4] and carbon nanotubes.[5–7] In recent years, polymer-based nanocomposites reinforced with expanded graphite (EG; also known as exfoliated graphite) have attracted a lot of attention because they show substantial improvements with small amounts of graphite not only in mechanical properties but also in electrical conductivity and barrier properties in comparison with the unmodified polymer.[8–12] A plausible reason for this is the sheetlike structure and multifunctional nature of graphite, along with its lower price.[13] Graphite is a naturally occurring or synthetically produced crystalline form of carbon that is highly conductive (with an electrical conductivity of 10^4 S/cm at the ambient temperature). EG is a graphite derivative obtained by the rapid heating of a graphite intercalation compound.[14] It exhibits a layered structure similar to that of layered silicate and is composed of stacks of nanosheets. The electrical conductivity of individual sheets and stacks of EG remains constant to some extent in comparison with the original graphite. More importantly, EG has a good affinity for both organic compounds and polymers; therefore, some monomers and polymers can be absorbed into the pores and galleries of EG.

The processing methods used for graphite-filled polymer nanocomposites are similar to the ones used for clays because both types of materials have layered structures, but some modifications are required because these two types of fillers are chemically different. After graphite is exfoliated through heat expansion, composites can be made through *in situ* polymerization, direct mechanical mixing, solution intercalation, and latex technology. Via *in situ* polymerization, in which the monomer is polymerized in the presence of graphite nanosheets, various polymer/graphite nanocomposites, such as poly(methyl methacrylate)/EG, polystyrene/EG, and nylon/EG, have already been achieved with very low percolation thresholds for electrical conductivity.[12,15,16] Direct mixing is widely used in polymer processing and theoretically can be used for most polymer systems, that is, low-viscosity thermoset matrices.[1,6] Solution intercalation is a method using a solvent to dissolve the polymer and disperse the graphite. The solvent is evaporated once the mixing is completed. Nanocomposites made by the solution

Correspondence to: M. Tian (tian71402@126.com).
Contract grant sponsor: National Natural Science Foundation of China; contract grant number: 50403029.

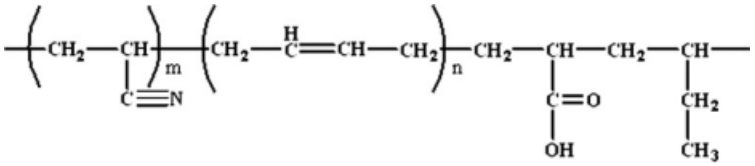

Figure 1 Chemical structure of xNBR.

approach include poly(methyl methacrylate)/EG[12,13] and maleic anhydride grafted polystyrene/EG.[16] This processing method results in nanocomposites with higher electrical conductivity and a lower percolation threshold in comparison with nanocomposites made from the exactly same materials with the direct-mixing technique.[16] However, rubber/graphite nanocomposites are rarely reported.[17,18]

The latex compounding method (LCM) is an innovative fabrication method for making polymer/inorganic filler nanocomposites in which a nanodispersed filler in water (requiring a surfactant) is mixed with a suspension of latex nanoparticles.[19] Because of its efficiency, simplicity, and environmentally friendly nature, LCM shows more promise for the large-scale output of polymer nanocomposites. This promising method is expected to be applied to polymers that can be synthesized by emulsion polymerization or formed into artificial latexes[20,21] and fillers that can be exfoliated/dispersed into nanounits in water media such as layered silicates. In our research group, various rubber/layered silicate nanocomposites with both mechanical properties and gas-barrier properties have been achieved through LCM.[2,22] On the basis of the LCM mechanism, we also prepared a nitrile rubber/EG composite that exhibited remarkably better mechanical properties and gas-barrier properties than a counterpart from direct mixing on a two-roll mill. It is important that LCM can avoid the fracturing of EG sheets in the course of shearing on a two-roll mill. We found that without any mixing under shear force, the nitrile rubber/EG composite made by LCM could display very good electrical conductivity with 10 phr graphite,[17] and the conductivity could be significantly reduced by the mixing process on a two-roll mill. The electrical conductivity properties and the structure of the polystyrene/EG composite were affected significantly by the rolling process.[16]

Carboxylated acrylonitrile butadiene rubber (xNBR)[23] is a copolymer containing at least one conjugated diene, one unsaturated nitrile, one carboxylated monomer, and optionally more comonomers. The chemical structure of xNBR is shown in Figure 1. It is an acrylonitrile butadiene rubber (NBR) elastomer improved through the addition of carboxylic acid groups to the NBR polymer backbone, which results in significantly increased strength, modulus, and abrasion resistance. In particular, the presence of chemically active functional groups (i.e., —COOH) in xNBR may make it easier for xNBR to interact with some fillers than NBR and ethylene propylene diene terpolymer.[24,25] It is not surprising that xNBR has found widespread use in the automotive (seals, hoses, and bearing pads), petroleum (stators, well head seals, and valve plates), electrical (cable sheathing), mechanical engineering (wheels and rollers), and shipbuilding (pipe seals and couplings) industries, among others. In previous research, it has been ascertained that the conventional direct-blending technique cannot ensure satisfactory dispersion of graphite nanolayers in a rubber compound,[17] whereas LCM is very effective in the nanoscale dispersion of graphite in rubber that possesses a latex or emulsion form. As a result, by LCM, the structural reinforcement and multifunctional nature of graphite nanosheets can be used to full effect in rubber nanocomposites. This study was intended to systematically investigate the mechanical properties, gas-barrier properties, and dielectric properties of EG-filled xNBR as a function of the filler concentration with LCM and achieve an improved xNBR composite for further applications.

EXPERIMENTAL

Materials

xNBR latex (Nantex 630C) was received from Nantex Industry Co., Ltd. (Taiwan Province, China). Expandable graphite (the expansion ratio along the *c* axis was ca. 250) was provided by Pingdu Huadong Graphite Processing Factory (Qingdao City, Shandong Province, China). Other chemicals, including rubber-curing additives, were bought from stores and used as received.

Preparation procedures

EG was prepared through the microwave irradiation of graphite oxide for about 30 s in a Sanyo EM-183MS1 microwave oven (Shanghai Yongle Household Electical Appliances Co., Ltd., Shanghai, China) with a power of 700 W at a frequency of 2.45 GHz, as described elsewhere.[26] Then, EG was mixed and saturated with deionized water with the aid of the

surfactant sodium dodecylsulfonate (SDS). In a typical procedure, an EG/SDS/H_2O ratio of 1 g/5 g/1.5 L was applied. The mixture was subjected to ultrasonic treatment with a power of approximately 100 W for 8 h, and a comparatively stable aqueous suspension of graphitic nanosheets was then formed. The xNBR latex was added to the suspension slowly under vigorous stirring and subsequently treated with ultrasonic irradiation for 30 min. Then, an aqueous $CaCl_2$ solution (1 wt %) was added to cocoagulate rubber and graphite to produce the nanocomposite compounds.

Vulcanizates of the nanocomposites were prepared by the addition of dicumyl peroxide (DCP) at the addition level of 4 phr. The blending process was carried out on a regular 6-in. two-roll mill. Then, about 7 g of the mix was tested in an oscillating disc rheometer to measure its optimum curing time (i.e., the time needed to achieve to 90% of the cure) at 160°C. Vulcanization of the samples was carried out with a press molding machine for the time needed to achieve 90% of the cure at 15 MPa and 160°C.

Characterization and tests

The morphologies of the freeze-fractured surfaces of the compounds were taken with an XL-30 high-definition environmental scanning electron microscope (ESEM) from Philips Electron Optics (USA). Transmission electron microscopy (TEM) observations were performed with a Hitachi (Japan) H-800 transmission electron microscope at an acceleration voltage of 200 kV.

The Shore A hardness of the vulcanizates was measured according to ASTM D 2240 with a XY-1 type A durometer (No. 4 Chemical Machinery Plant, Shanghai Chemical Equipment Co., Ltd., Shanghai, China), and three different spots of a sample (>6 mm thick) were measured to obtain an average value. Tensile testing of dumbbell specimens of the vulcanizates was carried out on a CMT4104 testing machine (Shenzhen SANS Testing Machine, Shenzhen, China) at a speed of 500 mm/min according to ASTM D 412. The storage modulus (E') and dynamic loss factor (tan δ) as a function of temperature were measured with a DMTA V dynamic mechanical thermal analyzer (Rheometrics Science Corp., USA) under the tension mode at 1 Hz and 3°C/min.

Nitrogen permeation tests were performed with a gas permeability measurement apparatus described elsewhere.[4] Bulk electrical conductivity tests were conducted with a Zheng-Yang model QJ84 ohmmeter (Shanghai Zhengyang Instrument Factory, Shanghai, China) with a four-terminal measurement feature to determine the bulk conductivity. Wear properties were evaluated with a ring-on-disc tester (manufactured by Jinan Shijin Co., China).[18,27]

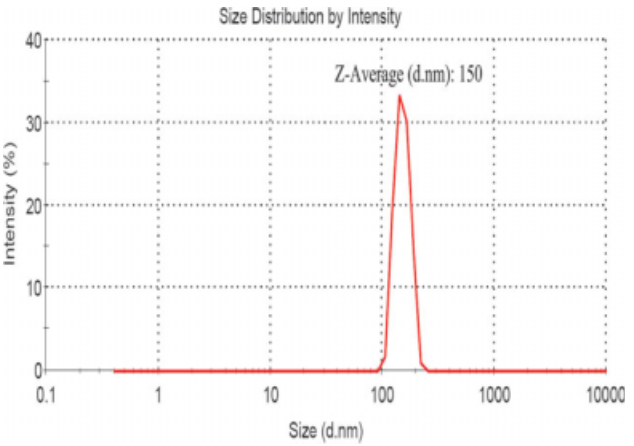

Figure 2 Size distribution of the rubber particles in the xNBR latex. [Color figure can be viewed in the online issue, which is available at www.interscience.wiley.com.]

RESULTS AND DISCUSSION

Morphology of the nanocomposites

The size distribution of the xNBR latex particles is displayed in Figure 2, and the average particle size was around 150 nm. Graphite nanosheets were obtained through the thermal decomposition of graphite oxide and subsequent ultrasonic treatment, as described elsewhere.[28] Those graphite nanosheets possessed nanometer-scale thickness but had quite large surface dimensions, usually several to tens of micrometers, as shown in Figure 3(a). Because EG agglomerates could be exfoliated into lots of nanosheets with the aid of water and ultrasonic stirring and then the surfactant SDS was added to stabilize the aqueous suspension, it was very easy to obtain a nanodispersion of the graphite and rubber through the mixing of the nanosheet suspension with the xNBR latex. After the drying of the nanocompounds in an oven, samples with different amounts of EG were prepared for scanning electronic microscopy (SEM) observation, as shown in Figure 3(c–e). In comparison with neat xNBR [Fig. 3(b)], many finely dispersed EG sheets (see the embedded white lines in Fig. 3) were found to accompany incompletely exfoliated agglomerates on the freeze-fractured surfaces of the xNBR/EG composites. As the amount of EG increased, the accompanying incompletely exfoliated agglomerates seemed more numerous. Also, some holes were observed, in that those agglomerates were pulled out from the matrix, especially at the EG concentration of 10 phr. The composite with 5 phr EG exhibited better dispersion of EG and graphite filler/xNBR interface adhesion than the composite with 10 phr. Similarly to NBR/EG nanocomposites,[17] EG–xNBR adhesion was achieved when EG was nanodispersed. By TEM, the

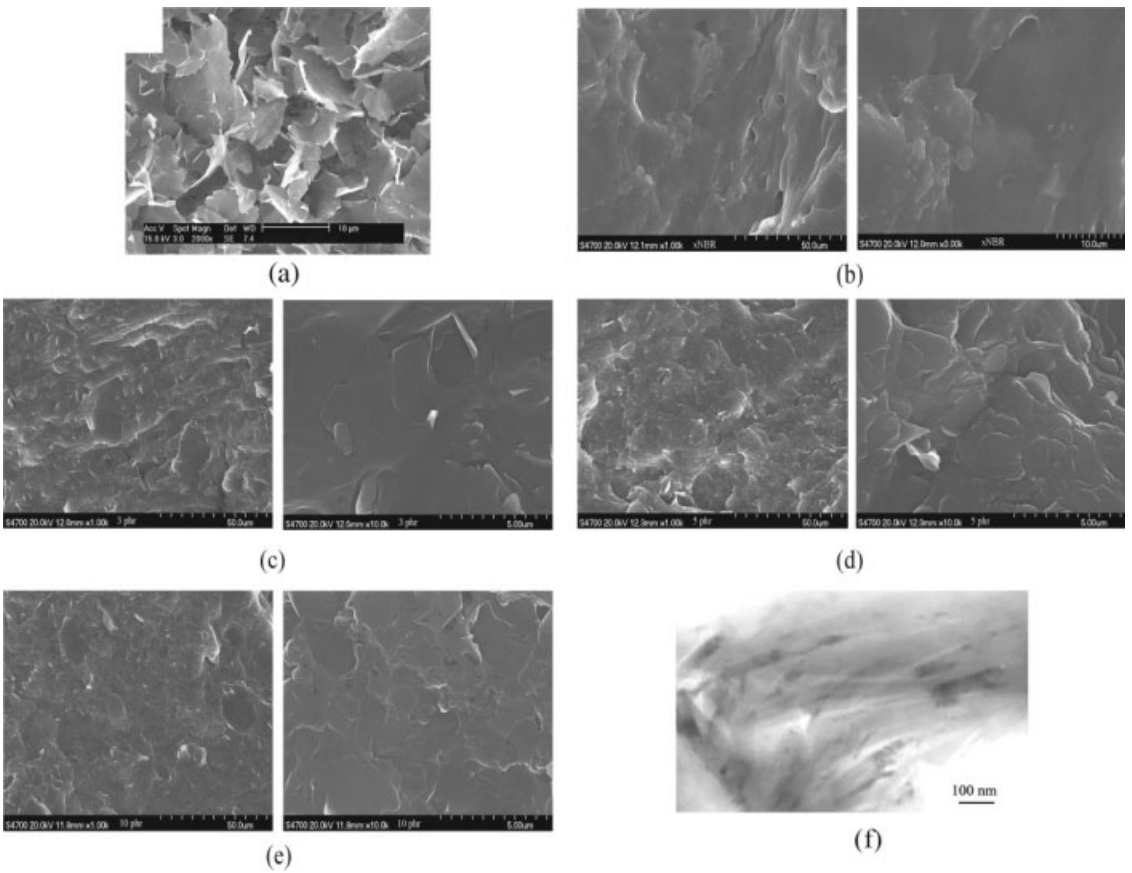

Figure 3 (a) SEM micrograph of the EG powder pretreated with ultrasonic irradiation, (b) SEM micrograph of the neat XNBR, (c–e) SEM micrographs of the xNBR composites filled with different amounts of EG (3, 5, or 10 phr) prepared by latex compounding, and (f) TEM image of the xNBR nanocomposite with 5 phr EG.

nanometer thickness of the dispersed graphite could be observed [Fig. 3(f)].

X-ray diffraction (XRD) analysis

The microstructure of the xNBR/EG nanocomposites prepared by LCM was further studied with XRD, which revealed the coexistence of intercalated and exfoliated microstructures (see Fig. 4).

Figure 4(a) shows the XRD patterns of EG powder after the ultrasonic treatment with surfactant SDS. The diffraction peak at $2\theta = 26.6^\circ$ corresponded to a basal spacing of 0.335 nm, which is the lamellar characteristic of graphite. However, with ultrasonic treatment, nanometer-thick graphite sheets could be obtained in the aqueous suspension, and those sheets were covered by surfactant molecules. After the addition of xNBR, the latex particles entered the sheet network in suspension, and graphite sheets were separated by strong ultrasonic irradiation. During subsequent flocculation, the flocculant caused the xNBR macromolecules and graphite sheets to flocculate simultaneously, and a nanoscale dispersion of graphite nanosheets was hence maintained in the xNBR matrix. Therefore, the diffractions of

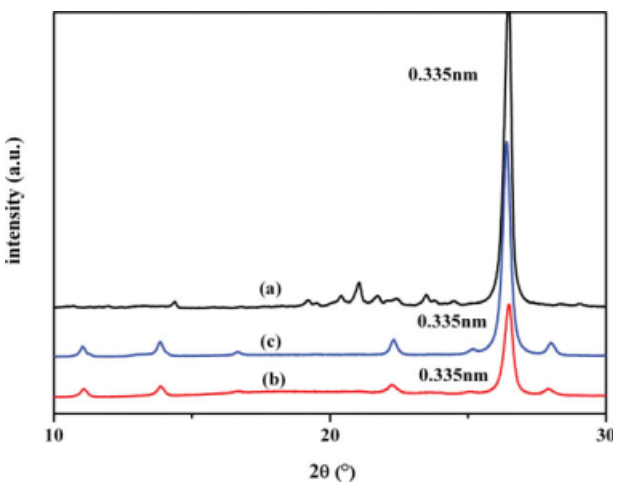

Figure 4 XRD patterns of (a) the EG powder pretreated with ultrasonic irradiation and dried with intercalated SDS, (b) the xNBR/5 phr EG nanocomposite prepared by latex compounding, and (c) the xNBR/20 phr EG nanocomposite prepared by latex compounding. [Color figure can be viewed in the online issue, which is available at www.interscience.wiley.com.]

TABLE I
Mechanical Properties of the Graphite-Filled xNBR Vulcanizates

	Sample			
	X0	X5	X10	X20
Graphite content (phr)	0	5	10	20
Shore A hardness	64	66	70	80
Stress at 100% elongation (MPa)	1.3 ± 0.1	2.4 ± 0.2	3.8 ± 0.1	6.3 ± 0.2
Stress at 300% elongation (MPa)	3.2 ± 0.2	4.7 ± 0.6	6.1 ± 0.3	—
Tensile strength (MPa)	7.4 ± 0.5	12.2 ± 1.6	10.7 ± 1.0	11.7 ± 1.0
Elongation at break (%)	590 ± 40	590 ± 50	530 ± 30	280 ± 30
Permanent tensile set (%)	2	8	20	36
Density (g/cm^3)	1.02	1.04	1.06	1.10

graphite at $2\theta = 26.6°$, corresponding to a basal spacing of 0.335 nm, were much weaker in the nanocomposites prepared by LCM and especially in the composite with 5 phr EG, as shown in Figure 4(b,c). When the loading amount of EG was 20 phr, the peak at $2\theta = 26.6°$ became stronger, and this indicated more unexfoliated EG. These observed results indicate that LCM produces a greater extent of exfoliation and a uniform dispersion of graphite nanosheets in the xNBR matrix but also incompletely exfoliated agglomerates.

Mechanical properties

The effects of the graphite content on the mechanical properties of the xNBR vulcanizates are summarized in Table I, and the tensile stress–strain behaviors of the xNBR vulcanizates are displayed in detail in Figure 5.

As is well known, when a hard phase is incorporated into a soft elastomeric matrix, the hardness of the elastomer usually will increase. Table I shows that the hardness of the vulcanizates steadily increased with the graphite content increasing. The stress (tensile modulus) at a certain elongation (e.g., 100 or 300%) of the vulcanizates also improved substantially when the graphite loading level increased in the range of 0–20 phr. However, the tensile strength increased rapidly with the concentration of graphite increasing from 0 to 5 phr, but less with a greater graphite loading. As observed previously, these unexfoliated agglomerates caused more stress concentration, which resulted in reduced elongation at break and limited tensile strength. For the same reason, more detachment of the interface took place with the tensile deformation and material break, and this was not recoverable after the tensile force was removed. Thus, the permanent set of the materials increased with increasing graphite content, as indicated in Table I. On the whole, once the filler could be dispersed as nanosized units in the rubber, the filler–rubber interface adhesion was improved, in that the nanofiller showed a large surface area. On the other hand, as more nanofiller was added, it was more difficult to disperse it into nanosized units in the rubber matrix.

From the stress–strain curves (Fig. 5), it can be clearly seen that with the increase in the graphite content from 0 to 20 phr, the slope of the curve in the initial stage increased significantly, and the material became much stiffer and stronger than very soft neat xNBR. This high reinforcement by graphite nanosheets was very distinct, and it may be attributed to the nanoscale uniform dispersion of graphite as well as the large aspect ratio of the layered structure, which was similar to a nanoclay filler.

Dynamic mechanical properties

Figure 6 shows the temperature dependence of E' and tan δ of the graphite-filled xNBR nanocomposites.

E' at a given temperature above the glass-transition temperature (T_g) increased with increasing

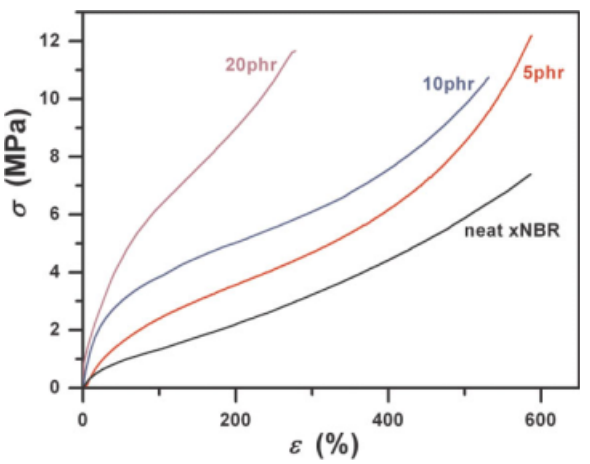

Figure 5 Tensile stress (σ)–strain (ε) curves of the graphite-filled xNBR composites. [Color figure can be viewed in the online issue, which is available at www.interscience.wiley.com.]

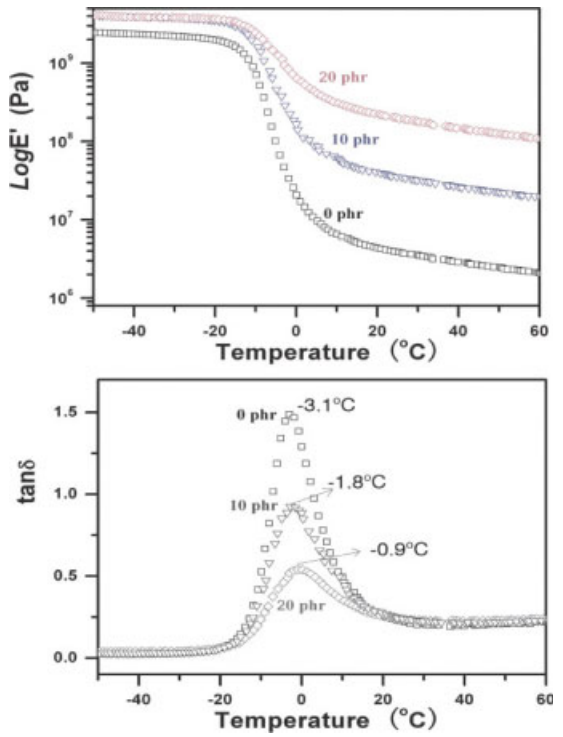

Figure 6 Effects of the graphite loading on E' and tan δ of the xNBR composites. [Color figure can be viewed in the online issue, which is available at www.interscience.wiley.com.]

graphite content. The plateaulike behavior of E' of the xNBR nanocomposites with graphite exhibited an enhancement of E' in comparison with E' of pure xNBR in the same temperature range. A similar trend for the dynamic mechanical properties has been observed in other rubber composites filled with reinforcing fillers such as clay.[29–31] Because the neat rubber material, having a relatively low modulus, is usually very soft, when a strong filler network is formed in the matrix, the improvement in the modulus is quite distinct.

The peak point of tan δ (this temperature is called T_g) was slightly shifted to a higher temperature, in comparison with pure xNBR, with increasing graphite content. This means that T_g increased in comparison with that of pure xNBR because the chain mobility of the xNBR chain segments was restricted near the filler surface. The change in T_g obtained from tan δ is also shown in Figure 6. However, T_g, which was determined from the peak point of tan δ, seemed to be nearly unvaried with increasing graphite content. From this result, it is more appropriate to mention that the incorporation of graphite had a minor effect on the increase in T_g of the rubber composite. The phase shift in a dynamic mechanical thermal analysis experiment is expressed as damping tan δ. The peak area under the tan δ curve at the glass transition, for example, is a measure of the energy that has dissipated during the dynamic experiment and gives information about the viscous parts of the nanocomposites. There was a large decrease in the peak area under the tan δ curve for all filled systems in comparison with pure xNBR. This means that the damping was reduced with increasing graphite content. At the glass-transition region of rubber, the hysteresis loss of the composite dominantly resulted from the elastic viscosity of rubber. The shifting and broadening of the tan δ peak toward higher temperatures for the nanocomposites indicated an increase in T_g together with some broadening of this transition. It can be explained as follows: the motion of a few rubber macromolecular chains at the organic–inorganic interface region was restricted, and this was somewhat different from free macromolecular chains.

TABLE II
Gas (N_2) Permeability of the Graphite-Filled xNBR Vulcanizates

	Sample				
	X0	X3	X5	X10	X20
Graphite content (phr)	0	3	5	10	20
N_2 permeability (10^{-18} m^2 Pa^{-1} s^{-1})	6.64	5.45	3.20	3.02	2.01

Gas-barrier properties of the nanocomposites

Soft, rubbery materials usually have very low gas-barrier properties because of the large free volume in comparison with plastics. The reduction of permeability arises from the longer diffusive path that the penetrants must travel in the presence of the filler, and the sheetlike morphology that graphite nanosheets also display in the nanocomposites is particularly efficient at maximizing the tortuous path for a diffusing penetrant. The gas permeability of the neat

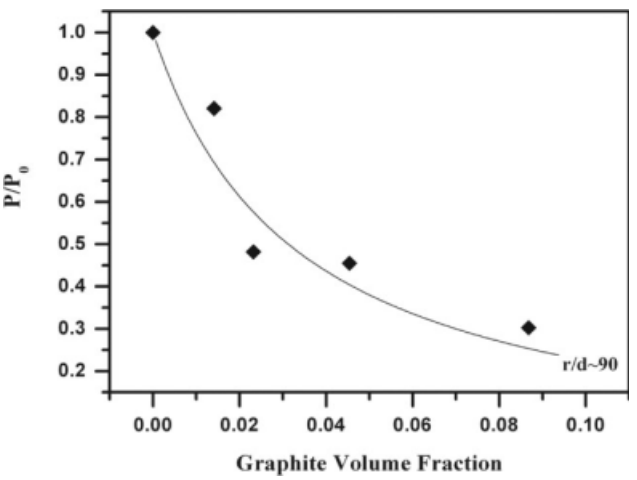

Figure 7 Gas (N_2) permeability of the graphite-filled xNBR composites.

TABLE III
Electrical Conductivity of the xNBR/Graphite Nanocompounds After Cocoagulation

	Graphite content (phr)				
	0	3	5	10	20
Electrical conductivity (S/cm)	Nonconductive[a]	Nonconductive	Nonconductive	0.2 ± 0.03	2.4 ± 0.2

[a] The conductivity could not be detected by the instrument used in this experiment ($<10^{-4}$ S/cm).

xNBR vulcanizate and xNBR/graphite nanocomposites with different graphite contents are presented in Table II. The nitrogen permeabilities decreased significantly with the increase in the amount of the filler.

A simple two-dimensional model was developed by Neilson[32] to predict the barrier performance of polymer composites containing platelet particles strictly on the basis of tortuosity arguments, and it was further developed with consideration of the dependence of the tortuosity factor on the orientational order of the sheets in a continuous manner. It can be argued that the distribution of graphite nanosheets in the xNBR matrix is uniform according to the study of the nanocomposite morphology, and if we assume that the orientation of the nanosheets is in a random mode, the following equation can be used to model the dependence of the relative gas permeability (P/P_0, where P is the gas permeability and P_0 is the initial gas permeability) on the filler volume fraction (ϕ) and the aspect ratio ($2r/d$, where r is the radius of the nanosheets and d is the thickness):[33]

$$P/P_0 = \frac{1 - \phi}{1 + (r/d)(\phi/3)} \quad (1)$$

The volume fraction of graphite was calculated with the densities of the neat xNBR vulcanizate and xNBR/graphite nanocomposites, which were measured via the weighing of a piece of the sample in air and in ethanol, and with an approximate density of compressed graphite nanosheets of 2 g/cm^3. P/P_0 (N_2) for the xNBR/graphite composites as a function of the volume fraction of graphite is displayed in Figure 7. As shown in Figure 7, the xNBR/graphite composites showed a rapid decrease in N_2 permeability at low loading levels, and this leveled off with further increases in the graphite volume. In addition, the experimental data are well located around the line predicted by eq. (1) with the value of r/d at 90, and this indicates that the average aspect ratio of the graphite nanosheets was about 180 (90×2). The actual value was less because the graphite nanosheets partially took an orientation perpendicular to the direction of gas diffusion during the sample preparation with a hot press, and this was also beneficial for the gas-barrier properties. According to the microscope study of the graphite nanosheet and composite morphologies in the previous discussion, the nanosheets had a thickness around 50–100 nm and a width around 10 μm; this meant an aspect ratio of about 100–200 for the graphite filler, which is in accordance with the modeling result from eq. (1).

Electrical conductivity

The incorporation of conductive fillers, such as metal particles, carbon black, carbon fibers, carbon nanotubes, and graphite, into a polymer matrix provides opportunities for attaining composites with high dielectric constants, conductivity, or capacitance. Table III shows that, when the loading level of EG exceeded 10 phr, the compound, which was available after cocoagulation during latex compounding, showed very good electrical conductivity. We found that the electrical conductivity disappeared after just the compound was mechanically mixed with the other compositions. It seems that the orientation of the EG nanosheets and sample preparation had a big impact on the conductive network of the filler and further affected the electrical and dielectric properties of the composites.

Friction and wear properties

As shown in Table IV, the addition of graphite also greatly enhanced the wear properties of xNBR in terms of the friction coefficient and wear rate. In comparison with neat xNBR, although the friction coefficient of the composites decreased little, the wear rate greatly decreased. At the loading of 20 phr, the composite showed a very low wear rate (only 6.1×10^{-5} mm^3/N m), which was reduced by 1000 times in comparison with neat xNBR. The

TABLE IV
Friction Coefficients and Wear Rates of the Graphite-Filled xNBR Vulcanizates

Graphite content (phr)	Friction coefficient	Wear rate (mm^3/N m)
0	1.5 ± 0.06	4.6×10^{-2}
5	1.4 ± 0.07	1.3×10^{-3}
10	1.3 ± 0.02	2.5×10^{-4}
20	1.1 ± 0.03	6.1×10^{-5}

improved wear property is very significant and desirable for rubber seals in dynamic use.

CONCLUSIONS

xNBR/EG nanocomposites were prepared through the blending of an aqueous EG suspension and xNBR latex by ultrasonic stirring. As the EG loading level did not exceed 5 phr, the dispersion (exfoliation) of EG and the filler–rubber interface adhesion were better. The mechanical behavior of the composites was greatly improved with the EG loading increasing, and this resulted from the large aspect ratio of the layered structure and the uniform dispersion of EG. Because of the functionality of EG itself, the graphite-filled xNBR composites also showed evident electrical conductivity as well as excellent gas-barrier and wear properties.

References

1. Messersmith, P. B.; Giannelis, E. P. Chem Mater 1993, 5, 1064.
2. Giannelis, E. P. Adv Mater 1996, 8, 29.
3. Ray, S. S.; Okamoto, M. Prog Polym Sci 2003, 28, 1539.
4. Wu, Y. P.; Wang, Y. Q.; Zhang, H. F.; Wang, Y. Z.; Yu, D.; Zhang, L. Q.; Yang, J. Compos Sci Technol 2005, 65, 1195.
5. Ajayan, P. M.; Zhou, O. Z. Top Appl Phys 2001, 80, 391.
6. Dai, L.; Mau, A. W. H. Adv Mater 2001, 13, 899.
7. Coleman, J. N.; Khan, U.; Gun'ko, Y. K. Adv Mater 2006, 18, 689.
8. Du, X. S.; Xiao, M.; Meng, Y. Z. J Polym Sci Part B: Polym Phys 2004, 42, 972.
9. Lu, J. R.; Weng, W.; Chen, X. F.; Wu, D. J.; Wu, C. L.; Chen, G. H. Adv Funct Mater 2005, 15, 1358.
10. Jia, W.; Tchoudakov, R.; Narkis, M.; Siegmann, A. Polym Compos 2005, 26, 526.
11. Chen, G. H.; Wu, D. J.; Weng, W. G.; Yan, W. L. J Appl Polym Sci 2001, 82, 2506.
12. Pan, Y. X.; Yu, Z. Z.; Ou, Y. C.; Hu, G. H. J Polym Sci Part B: Polym Phys 2000, 38, 1626.
13. Chung, D. D. L. J Mater Sci 2002, 37, 1475.
14. Schaufhautl, P. J Prakt Chem 1841, 21, 55.
15. Chen, G. H.; Weng, W. G.; Wu, D. J.; Wu, C. L. Eur Polym J 2003, 39, 2329.
16. Chen, G. H.; Wu, D. J.; Weng, W. G.; He, B.; Yan, W. L. Polym Int 2001, 50, 980.
17. Yang, J.; Tian, M.; Jia, Q. X.; Shi, J. H.; Zhang, L. Q.; Lim, S. H.; Yu, Z. Z.; Mai, Y. W. Acta Mater 2007, 55, 6372.
18. Yang, J.; Tian, M.; Jia, Q. X.; Zhang, L. Q.; Li, X. L. J Appl Polym Sci 2006, 102, 4007.
19. Wu, Y. P.; Qi, Q.; Liang, G. H.; Zhang, L. Q. Carbohydr Polym 2006, 65, 109.
20. Zhang, L. Q.; Wang, Y. Z.; Wang, Y. Q.; Sui, Y.; Yu, D. S. J Appl Polym Sci 2000, 78, 1873.
21. Wu, Y. P.; Ji, M. Q.; Qi, Q.; Wang, Y. Q.; Zhang, L. Q. Rapid Commun 2004, 25, 565.
22. Jia, Q. X.; Wu, Y. P.; Wang, Y. Q.; Lu, M.; Zhang, L. Q. Compos Sci Technol 2008, 68, 1050.
23. Lu, L.; Zhai, Y. H.; Zhang, Y.; Christopher, O.; Sharon, G. Appl Surf Sci 2008, 255, 2162.
24. Chronska, K.; Przepiorkowska, A. J Hazard Mater 2008, 51, 348.
25. Pradhan, S.; Costa, F. R.; Wagenknecht, U.; Jehnichen, D.; Bhowmick, A. K.; Heinrich, G. Eur Polym J 2008, 44, 3122.
26. Chung, D. D. L. J Mater Sci 1987, 22, 4190.
27. Bieliński, D.; Ślusarski, L. Wear 1993, 169, 257.
28. Chen, G. H.; Weng, W. G.; Wu, D. J.; Wu, C. L.; Lu, J. R.; Wang, P. P. Carbon 2004, 42, 753.
29. Kim, J.; Oh, T.; Lee, D. Polym Int 2003, 52, 1058.
30. Liu, L.; Jia, D.; Luo, Y.; Guo, B. J Appl Polym Sci 2006, 100, 1905.
31. Shokri, A. A. Polym Int 2006, 55, iii.
32. Neilson, P. D.; Neilson, M. D. Hum Movement Sci 2004, 23, 278.
33. Nagaki, M.; Suwa, T. Carbon 2001, 39, 915.